Tellus (2002), 54A, 370–381

TELLUS
ISSN 0280–6495

Hydrometeor structure of a composite monsoon depression using the TRMM radar

By GEOFFREY STANO, T. N. KRISHNAMURTI*, T. S. V. VIJAYA KUMAR and ARUN CHAKRABORTY, *Department of Meteorology, Florida State University, Tallahassee, FL32310, USA*

(Manuscript received 2 July 2001; in final form 11 February 2002)

ABSTRACT

This paper addresses the use of a satellite-based radar for obtaining the composite structure (from several monsoon depressions) of the distribution of precipitation elements in the horizontal and the vertical. This composting is based on the use of a simple elliptical layout of coordinates along the major and minor axes of each storm as it passed over north central India. This satellite, called the Tropical Rainfall Measuring Mission (TRMM), carries onboard a microwave instrument known as the Precipitation Radar (PR). The vertical structure of hydrometeors provided by the radar is somewhat of the same quality as the ground-based Doppler radar units. The PR could identify many features such as the melting layers, height of convection, extent of anvils and types of precipitation over different sections of the composited monsoon depression. Furthermore, the asymmetric nature of surface rainfall that intensifies around the composited monsoon depression has also been mapped, which could provide several more details than was possible from other satellite-based estimates. It is found that the most intense precipitation occurs in the south-southwest region of the monsoon depression. The preponderance of stratiform rain and the coverage of fewer deep convective elements, especially over the orographic upslope region, are some other noticeable features obtained using the TRMM PR. The stratiform rain was noted to arise where the melting layers (in the radar reflectivity signatures) were located near 5 km. In those few occasions where tall rain clouds were discernible, the cloud tops were seen to extend all the way from 12 to 15 km. Rainfall amounts across the composite monsoon depression range from 10 to 100 mm d^{-1}. The 3–4 d passage time of one of those disturbances resulted in local rainfall totals of the order of 200–300 mm d^{-1}.

1. Introduction

Through this paper we wish to portray the hydrometeor structure of a composite monsoon depression over the Indian region for the year 1999. Such a structure has not been possible because of inadequate radar data coverage over the land areas. Although a few coastal radar units were available over the Arabian Sea and Bay of Bengal, these did not have a range to cover the entire scale of a monsoon depression, which is of the order of 3000 km.

The monsoon depression is an important synoptic feature, which accounts for a significant amount of monsoon rains over the Indian subcontinent. These systems of low pressure generally have two to three closed isobars with 2 hPa intervals and occur between the months of June to September. These generally form in the Bay of Bengal north of 18°N. The overall motion of these systems is to the west-northwest, and the storms can persist into the central parts of India for 2–4 d prior to

* Corresponding author.
e-mail: tnk@io.met.fsu.edu

weakening. The upper air circulation of these systems extends to 500 hPa and also up to 300 hPa occasionally. The lowest temperatures found in the depression are thought to be in the southwest quadrant up to about 700 hPa. This is due in part to the monsoon air flowing into this part of the system being lifted in the zone of heavy rains (Rao, 1976). Other common features of monsoon depressions include an extensive heavy overcast cloud mass located in its southern and western sectors. This cloud mass has an extent of five to seven degrees of latitude. The northern sector of the system in many cases includes cumuliform clouds, which organize into bands as the depression strengthens. Previous research indicates that the heaviest rains in a monsoon depression are located to the west of the storm's center. Elsewhere, the rainfall amounts are generally quite small, despite the fact that the monsoon depression is a tropical low (Rao, 1976). This finding is further supported by rainfall composites by Bedekar and Banerjee (1969), Krishnamurti et al. (1975) and Godbole (1977), who found that heavy rainfall was concentrated to the left of the track of the monsoon depression. The Tropical Rainfall Measuring Mission (TRMM) satellite, launched jointly by NASA and NASDA on 27 November 1998, provided a unique opportunity for compositing the hydrometeor structure from the use of the TRMM radar (called the Precipitation Radar, PR). A list of acronyms used in this paper is given in Table 1. Attempts have been made by some researchers (Short and Nakamura, 2000; Liu and Fu, 2001) to study the characteristics of tropical precipitation profiles using TRMM satellite radar measurements.

Table 1. *List of Acronyms*

BB	Bright Band
CERES	Cloud and Earth Radiation Energy System
DMSP	Defense Meteorological Satellite Program
GHz	Giga Hertz
IMD	India Meteorological Department
LIS	Lightning Imaging Sensor
NASA	National Aeronautics and Space Administration
NASDA	National Space Development Agency of Japan
OLR	Outgoing Longwave Radiation
PR	Precipitation Radar
SSMI	Special Sensor Microwave Imager
TMI	TRMM Microwave Imager
TRMM	Tropical Rainfall Measuring Mission
UTC	Universal Time Constant
VIS	Visible and Infrared Scanner

The importance of this study for the modeling community is obvious. Knowledge of the horizontal and vertical distribution of hydrometeors from such radar observations on the distributions of convective and non-convective components would assist in the numerical modeling of precipitating systems. Current cumulus parameterization schemes need to be tested on a number of such storms, and can further be improved from such composite radar signatures. That can be thought of as an objective of this study. Because of the limited nature of this short contribution the scope of this study would only be restricted to the radar composite structure of monsoon depressions.

This is a first study of its kind on the radar coverage over land areas of the monsoon depression. The coastal areas of India have inadequate coverage of radar units. The TRMM satellite provided a first opportunity to examine the precipitation structure in three dimensions over northern India, where the passage of these distributions has been known to produce heavy rainfall similar to that for the passage of hurricanes, i.e., about 300–500 mm of rain during individual disturbances.

2. Observations

The TRMM satellite has been designed for scientists and researchers to understand the properties of tropical rain on the Earth's climate through remote sensing. This satellite is in a low-earth orbit approximately 350 km above the surface. The sinusoidal orbital path ranges approximately from 35°S to 35°N latitude. The low orbit permits a greater resolution of rainfall features near the Earth's surface. The TRMM satellite has five main onboard instruments. First is the Precipitation Radar (PR). This is the first such radar that is capable of measuring rainfall from space (Simpson et al., 1988). In principle, three-dimensional views of the structure of weather phenomena can be created from the measurements from this instrument. Second is the TRMM Microwave Imager (TMI), which is an instrument very similar to a microwave imager onboard the

US Air Force DMSP satellite called SSM/I. The microwave imager is a passive sensor able to measure microwave radiation at different wavelengths emitted by objects such as the land and the oceans, more importantly, clouds and precipitation, based on the temperatures of the objects. These are the two instruments that are being used in the present study. The other three instruments on the TRMM satellite include the Visible and Infrared Scanner (VIS), Cloud and Earth Radiation Energy System (CERES), and the Lightning Imaging Sensor (LIS).

Datasets from TRMM PR incorporate the satellite swaths and information on the vertical cross-sections of hydrometeors. This instrument measures backscattered radio wave signal strength from hydrometeors as the radar signal travels through clouds to the land or ocean and back to the TRMM satellite. The PR has a data swath width of 215 km. The observation band frequency, which has two-channel agility, is 13.796 and 13.802 GHz. This allows a cross-track scanning over a swath width of roughly 4.3 km. In addition to this, it has an instantaneous field of view horizontal resolution of 5 km or better (Simpson et al., 1988). The precipitation radar attempts to maintain a calibration to 1 dB. This instrument has 80 separate levels for vertical profiles (TRMM, 1996). The resolution of the data slightly depends on the scan angle of the satellite. This instrument is designed to resolve rain rates of the order of 0.7 mm h^{-1} with a range resolution of 250 m (Kozu et al., 2001).

For the 1999 monsoon season, there were three depressions, all of which formed in the northwestern Bay of Bengal. A brief description of these depressions, as gathered from the information provided by India Meteorological Department, IMD (2000) is given below:

(a) *Deep depression over the Bay of Bengal, 17–18 June 1999*: This was a well marked low-pressure area which formed over the northwest Bay of Orissa — West Bengal coast on 16 June, intensified into a deep depression at 0600 UTC, 17 June, moved in a west-northwesterly direction and crossed the Orissa coast at 2100 UTC, 17 June. It later weakened and moved further inland in a west-northwesterly direction and dissipated.

(b) *Deep depression over the Bay of Bengal, 27–29 July 1999*: This was also formed as a well marked low-pressure area over the northwest Bay of West Bengal coast on 26 July. This system intensified into a deep depression at 1200 UTC on 27 July and moved in a northwesterly direction before crossing the West Bengal–Orissa coast on the morning of 28 July. Later it weakened, moved in a northwesterly direction and became a depression at 1200 UTC on 28 July. It further moved in a west-northwesterly direction and dissipated by the evening of 29 July over the Madhya Pradesh region.

(c) *Depression over northwest Bay of Bengal, 6–8 August 1999*: This formed as a well marked low pressure over the northwest Bay of North Orissa–West Bengal coast in the morning of 6 August. It concentrated into a depression by 1200 UTC on 5 August and moved in a west-northwesterly direction before crossing the West Bengal coast at 0300 UTC on 7 August. Later it continued to move in a west-northwesterly direction and dissipated near the northeast Madhya Pradesh region by the morning of 9 August.

It is clear from the above description that all these three depressions have more or less similar characteristics in terms of region of formation, movement, intensification, strength and lifetimes. The tracks of these depressions are given in Fig. 1.

The TRMM satellite viewed these three depressions during 17–18 June, 27–28 July, and 6–8 August. As stated earlier, the TRMM data are presented in swaths as the satellite makes its orbit around the Earth. This caused some problems, since it was difficult to maintain good coverage on a depression as it moved inland. However, 16 excellent satellite swaths of data sets were acquired from the precipitation radar as well as from the TRMM microwave imager for this region.

The principle objective of this study is to obtain the horizontal distribution of precipitation and the vertical distribution of hydrometeors (as seen from satellite radar reflectivity) for a land-based monsoon depression where conventional ground-based radar coverage is very limited.

3. Methodology

Two PR-based data sets were utilized in this present study, the 2A-25 PR profile data and the 2A-23 PR qualitative data. (This numerical nomenclature identifies the NASA data archives and would facilitate the researchers to access

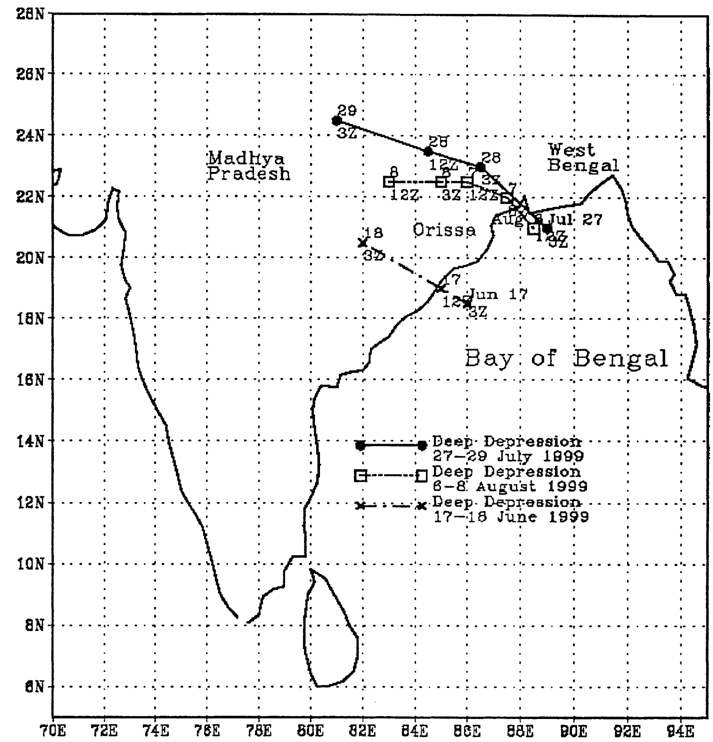

Fig. 1. Tracks of the monsoon depressions of 1999 over the Indian subcontinent.

TRMM data sets.) In the 2A-25 algorithm, the best estimate of the vertical rainfall rate profile for each radar beam is produced. The rainfall rate is given at each resolution cell of 4 km × 4 km × 250 m following a hybrid method described by Menighini et al. (1997) to estimate the true vertical radar reflectivity (Z) profile. The vertical rain profile is then calculated from the estimated true Z profile using an appropriate Z–R relationship. The rainfall composite image and the vertical cross-section images were derived from this dataset. The PR based 2A-23 algorithm attempts to qualitatively (1) detect the bright band, (2) determine the height of the bright band if it exists, (3) classify rain types, (4) output storm heights, and (5) output rain/no rain information. The bright band is detected by searching for peaks of Z-factor with respect to range. This peak search is made using a spatial filter, based on a second derivative concept. Whenever the peak is well defined and appears around the expected height of the freezing level, it is determined that the bright band exists and the height where the peak occurs is regarded as the height of the bright band (TRMM, 1996).

The 2A-23 uses two different methods for classifying rain type; one is vertical profile method (V-method), and the other is horizontal pattern method (H-method) (Awaka et al., 1998). Both methods classify rain into three categories; (1) stratiform, (2) convective, and (3) other. The V-method starts with a detection of the bright band (BB). The detection of the BB is made by a spatial filter which is based on the second derivative of Z with respect to range and by imposing several conditions on the BB, such as that Z above the BB peak should decrease appreciably, the height of the BB should appear almost at the same height, and so on. One of the major conditions imposed on the BB is that its height must be located in a BB window whose range is ± 1.5 km from height of freezing level estimated from a climatological surface temperature at sea level. After BB detection, the V-method classifies the rain type based on the following: (a) When a BB exists, rain is basically classified as stratiform. (b) When a BB is not detected, and the maximum value of Z at a given angle bin exceeds a convective threshold, the rain type for this angle bin is classified as convective. (c) 'Other' type is defined as not stratiform and not convective.

It should be noted that 'other' type of rain is defined by the V-method as not convective and not stratiform, which means there exists an appreciable radar echo which is not strong enough to be convective, and a BB is not detected.

The H-method also classifies rain into three categories: stratiform, convective, and other, but with the definitions of these being different from those of the V-method. The H-method is based on the University of Washington convective/stratiform separation method (Steiner et al., 1995), which examines the horizontal pattern of Z at a given height where Z has a 2 km horizontal resolution. In 2A-23, instead of examining a horizontal pattern of Z at a given height, a horizontal pattern of Z_{max} is examined; here, Z_{max} is the maximum of Z along the range for each antenna scan angle below freezH (minus 1 km margin), where freezH is the height of freezing level estimated from a climatological surface temperature at sea level, $T_{surface}$, by the formula $freezH = T_{surface}/T_{lapse}$, where T_{lapse} is the lapse rate of temperature. Parameters are changed so that they may be suitable for the TRMM data with 4.3 km horizontal resolution. 'Other' type of rain is introduced to handle noise. In the H-method, if Z_{max} exceeds a convective threshold, or Z_{max} stands out against the background area, the rain is classified as convective. If the rain type is not convective and if the rain echo is certain to exist, the rain type is classified as stratiform. The rain type is classied as 'other' if the radar echo below freezH (minus 1 km margin) at a given angle bin is possibly noise. This means that the 'other' type by the H-method includes the case of (i) noise and (ii) cloud. Detection of warm rain is also made in 2A-23.

The criteria for the definitions of stratiform and convective rain as seen from TRMM radar signatures, based on recent studies on TRMM PR by several scientists, e.g. Houze (1997) and Watson et al. (1988), are provided in Table 2.

Table 2. *Criteria for determining convective and stratiform rain as seen by TRMM radar*

Condition	Convective rain	Stratiform rain
Presence of light bands	×	√
Absence of bright bands	√	×
Reflection 20–40 dbz	√	√
Reflection >40 dbz	√	×
Presence of strong gradients of radar reflectivity	√	×
Absence of reflectivity gradients and reflection >20 dbz	×	√

The TMI-derived rain rates from the 2A-12 algorithm (Kummerow et al., 1996) were also used in this study to support the PR data. This algorithm makes use of cloud dynamical models. The TMI is a passive microwave sensor that is able to measure the outgoing microwave radiation from the Earth. This radiation is measured at 10.4, 19.4, 21.3, 37, and 85.5 GHz. The 10.4 GHz frequency was added to provide better results in areas of heavy tropical rainfall with a horizontal resolution of TMI 10 GHz is 63 km (across track) and 37 km (along track). The sensor is capable of detecting variables such as precipitable water over the oceans rather than over land due to the larger contrast in emitted radiation between the oceans and the land. Algorithms have been developed to compensate for this problem over land areas. The main technique is based upon a Bayesian approach in which many realizations of the Goddard Cumulus Ensemble model are incorporated to establish a prior probability density function of rainfall profiles. Detailed three-dimensional radiative transfer calculations are used to determine upwelling brightness temperatures from the cloud model to establish the similarity of radiative signatures and thus the probability that a given profile is actually observed. Improved results may be obtained by weighting the profiles from the prior probability density function according to the deviation from the observed brightness temperatures. Computationally, this is very quick, as this process avoids iterative radiative transfer computations. In addition, when the database of possible cloud structures is not sufficiently populated, a secondary approach developed by Ferraro et al. (1998) is used. Here, the profiles are adjusted using an iterative technique aimed at minimizing differences between observed and modeled brightness temperatures. This is computationally more intensive, but is only employed if no satisfactory results can be found by the primary method (TRMM, 1996). Since the PR has a data swath of only 215 km while the TMI has a data swath of 780 km, use of TMI data generally creates a superior overview of the synoptic rainfall events like a monsoon depression, but comes at the expense of a decrease in the resolution. Despite the problems associated with using the microwave imager over land, it has been included in this study to provide a contrast to the precipitation radar and to observe any features that the imager might detect.

The domain of this study includes the Indian subcontinent and the surrounding bodies of water. The exact coordinates for this domain are 60°E to 100°E longitude and from equator to 40°N latitude. The maximum area for a single TRMM image is a 40° latitude × 40° longitude domain, which allows inclusion of major synoptic level features such as the composite streamline analysis of the monsoon depressions. This study comprises the tracks and movements of all summer monsoon depressions during the 1999 monsoon season for the months between June and September described earlier in this paper. The 850 hPa streamline analyses for the selected dates were acquired from the FSU superensemble product (Krishnamurti et al., 2000). The circulation at 850 hPa typically identifies the strongest circulation of the monsoon depression. The composting is based on the use of a simple elliptical layout of coordinates along the major and minor axes of each storm as it passed over north central India.

For this study, the correct Z factor scan type algorithm that indicates the intensity of the storm was used. A single composite for all the depressions mentioned above was created and was overlaid with the 850 hPa streamline analysis. The streamlines serve as a guide for the depression's extent and shape. The selected domain consisting of these composite monsoon depressions was subdivided into different quadrants; specifically the left front, right front, right rear, and left rear quadrants relative to the composite system's center were examined as the systems moved roughly to the northwest. These quadrants made it possible to analyse the storm's intensity and overall rainfall relative to the depression's center.

The vertical cross-sections derived from the PR were used to prepare the composite of the Z factor data sets. These vertical cross-sections were made across areas of interest around the composite depression where some features such as bright banding and intense rain shafts were observed. These features helped to determine the types of water substance (liquid or ice) and led to the identification of the more intense convective sections of the monsoon depression. Supporting data for the cross-sections came from the qualitative 2A-23 data sets based on PR, which is used to analyze the bright band heights, freezing level, storm heights, and to determine if warm rain processes are occurring.

The microwave imager accomplishes some of the same scans as the PR with a larger spatial coverage, and hence only the composite rain map is prepared. The surface rain scan is used for a comparison against the precipitation radar's correct Z factor composite and for determining the types of precipitation processes that were occurring within the depression, i.e. stratiform or convective.

4. Results

The TRMM data indicate that the most intense precipitation of the depression is located in the left-front quadrant, roughly to the south-southwest of the system's center. In addition there is a large amount of precipitation ahead of the center of the system. The composite shows that, in fact, nearly all of the precipitation is in the left front quadrant. The exceptions to this are locations of precipitation induced by orographic lifting along the foothills of the Himalayas. This can be seen as a line of precipitation from 30°N, 78°E to 24°N, 93°E. In addition, there are small areas of precipitation over the Bay of Bengal and some heavier zones of precipitation along the land–sea interface in the eastern Bay of Bengal. The TMI data supports these findings from the PR.

It is difficult to assess how much qualitative improvement one can acquire from the use of the TRMM PR-based precipitation over those derived from the use of TMI algorithms or the classical OLR based algorithms. For comparison purposes we show the composite rainfall estimates derived from the TMI- and OLR-based algorithms for the monsoon depressions during 1999 in Figs. 2 and 3. These two rainfall products were prepared at

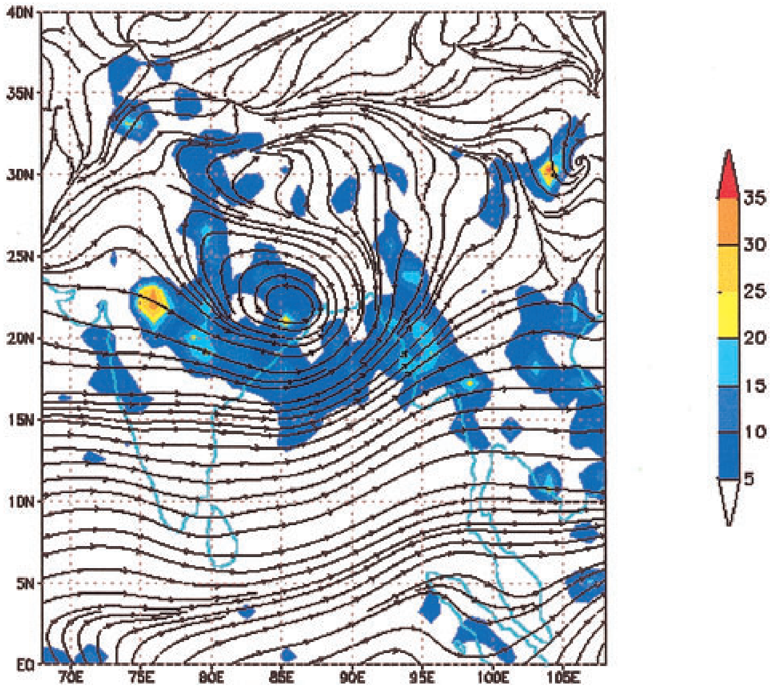

Fig. 2. Composite streamline analysis (850 hPa) + OLR-derived precipitation (mm d^{-1}) for the monsoon depressions of 1999. The OLR-derived precipitation data (Xie and Arkin, 1998) for the period of the three monsoon depressions is averaged and is displayed here. The streamlines are drawn using the composited real-time FSU superensemble data (Krishnamurti et al., 2000) for the period of the three monsoon depressions of 1999.

the resolution of approximately 80 and 150 km, respectively, for TRMM and OLR. We note that the sharpest rainfall signatures came from the use of the TRMM PR (also prepared at the resolution of about 80 km). The TMI-based rainfall product sees coarsest signatures of rain. The OLR-based rainfall derived from Xie and Arkin Global precipitation datasets (Xie and Arkin, 1998) includes several false returns from the overhanging cirrus (and related cold cloud tops), resulting in a rather broad/smeared rainfall distribution.

The main findings from this study are shown in Fig. 4, which is the composite of the TRMM PR images, with the vertical cross-sections identifying the heavy rain regions. This image shows one of the first composites of this type for the monsoon depression. The TRMM data appear to support several of the previous findings on the structure of monsoon depressions that were noted by Godbole (1973).

Here, the composite indicates that the majority of the precipitation comes from stratiform processes with isolated, intense convective cells embedded within. The stratiform rain is shown in the main composite image with dark colors. The yellows of the composite indicate heavier rains, while the dark oranges and reds indicate the areas of intense convective rain. The vertical cross-sections also show this basic structure. Cross-section (F) shows a strong convective cell indicated by the yellow core and the higher area of green in the center of the image. To the left of this cell is a larger area of stratiform rain with a small convective cell shown by the spike of vertically large amount of green. Surface meteorological data contain numerous reports of nimbostratus clouds over this region. Generally, the vertical cross-sections show mostly stratiform precipitation. Cross-section (A) is a good example of stratiform precipitation. The microwave imager's convective rainfall distribution also supports the scattered nature of the convective cells within the monsoon depression.

The next major feature shown by the composite

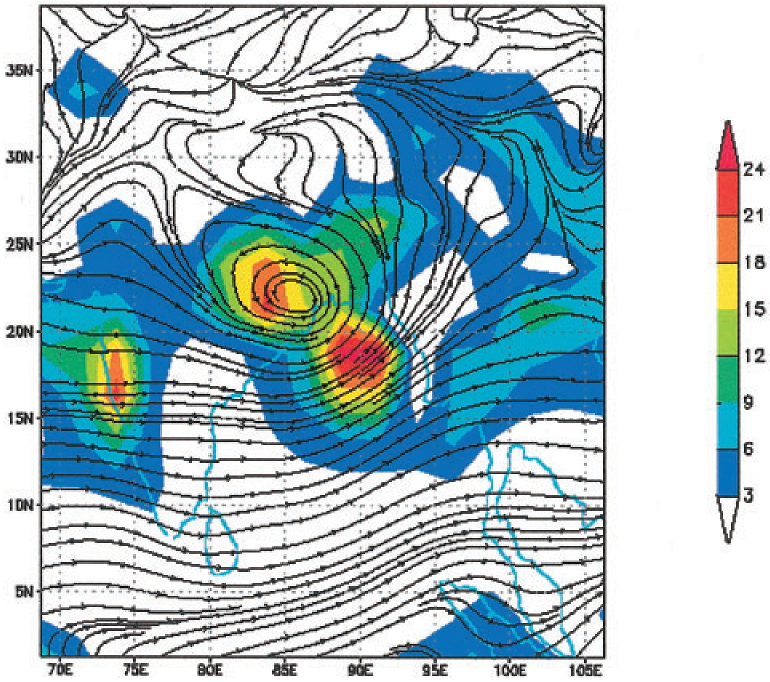

Fig. 3. Composite streamline analysis (850 hPa) + TRMM + SSM/I derived precipitation (mm d^{-1}) for the monsoon depressions of 1999. The TRMM-SSM/I-derived precipitation data come from the FSU multianalysis superensemble.

is the dry swath in the system to the north of the monsoon's track. This is bounded by the intense rains of the monsoon depressions' left-front quadrant and the orographically induced precipitation along the foothills of the Himalayas. Cross-section (H) indicates how the Western Ghats along the west coast of India also influence precipitation related to the passage of the monsoon depression. On the right side of (H) there is a strong area of precipitation, indicated by the green color. As the westerly wind flow encounters the elevated terrain, bright yellow coloring at the bottom right of the image identifies a heavy rain region.

An interesting note on the vertical cross-sections is the level of the bright band. Generally, the bright band is considered as the zone in the upper levels, which separates liquid water (below) and frozen water (above). The bright band can be found in the cross-sections by looking at the upper limit of the green areas of precipitation. The rightmost section of cross-section (E) shows a well defined bright band feature. Most of the cross-sections analyzed appear to have bright banding at a level 60, which according to the TRMM orbit viewer's vertical scale is an identifier. (The TRMM orbit viewer is data display software provided by NASA.) The vertical scale in the cross-sections increases downward with the surface (Earth's geoid) assigned a value of 79. The interval of the vertical scale is 250 m. The occurrence of bright banding and other notable features are discussed below where the individual cross-sections are presented. One of the other generalizations of all of the cross-sections is that the TRMM satellite did not delineate any warm rain processes.

Cross-section (A) depicts a region to the south-southwest of the monsoon depression's center. Using the TRMM Orbit Viewer for analyzing the 2A-23 data sets we find an approximate range of bright banding heights to lie between 4800 and 5100 m. The typical freezing level for this section is around 4720 m. There are also convective cell storm tops around 10 000 m, with the surrounding locations ranging in height from around 6600 to 8600 m. Along the eastern foothills of the Himalayan Mountains, cross-section (B) is shown to the northeast of the composite depressions. Here the approximate bright band height is

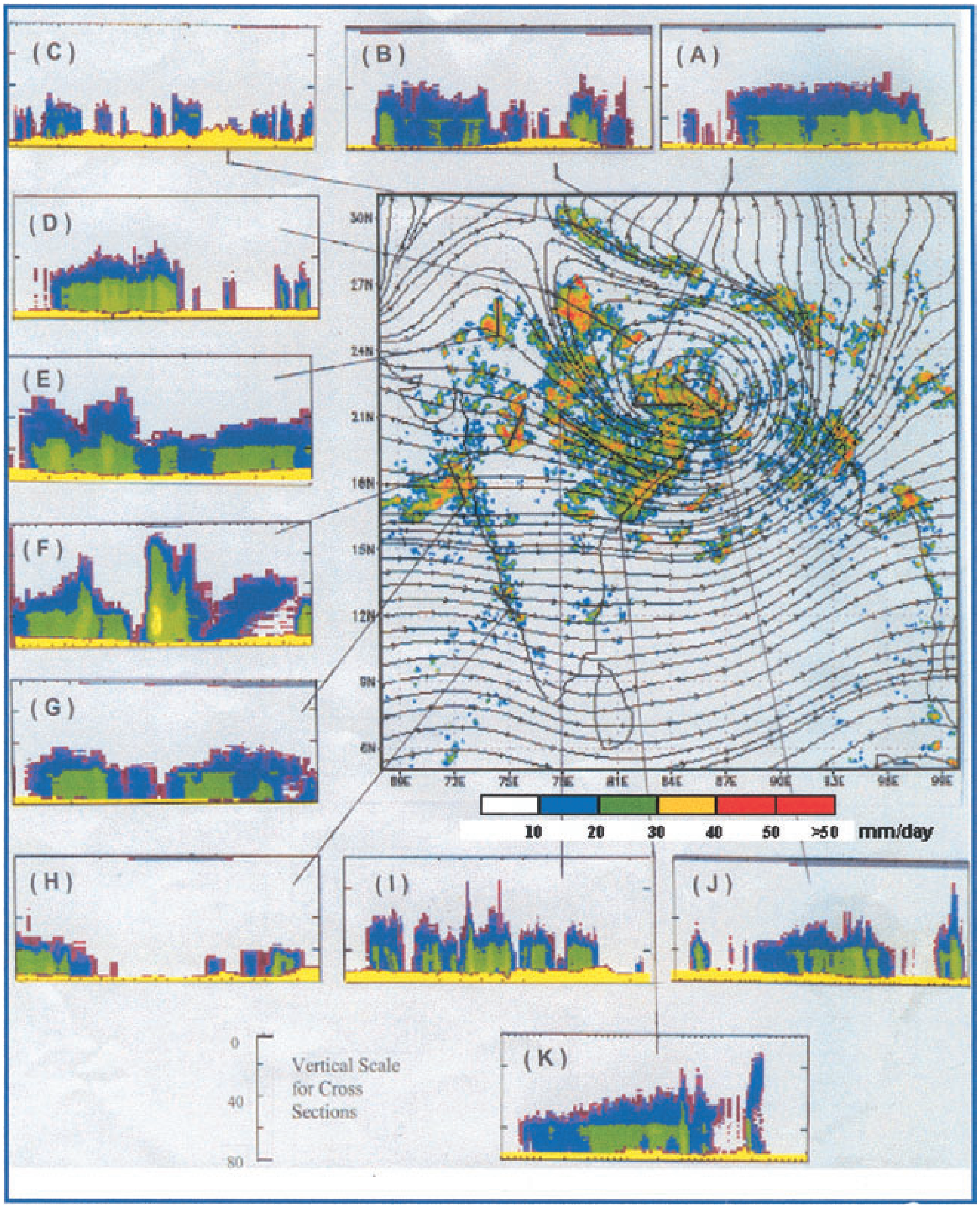

Fig. 4. Composite precipitation radar image with vertical cross-sections overlaid on the composite streamline analysis at 850 hPa for the monsoon depressions of 1999. The panels A–K show the vertical cross-sections from different parts of the rain areas of the composite monsoon depression. The PR- and TMI-derived composited precipitation (mm d^{-1}) is superimposed on the composited 850 hPa streamline analysis. The color bar shows the range of precipitation while the vertical scale depicts the range of the vertical cross-section of hydrometeors.

around 5000 m, with a freezing height of 4550 m. There are isolated convective cells with storm heights of the order of 10 100 m and 12 100 m, respectively. The rest of the location ranges from 6100 to 8200 m, signifying the presence of nimbostratus clouds.

Cross-section (C) also depicts features over the Himalayan foothills to the north and north-northeast of the composite storm center. The bright band locations are isolated due to the extreme height of the mountains. However, where clear readings occurred, the bright band height is near 5000 to 5300 m with a freezing level near 4200 m. The storm heights in this region are not as intense as many others, but still range from 5700 to 6400 m.

Cross-section (D) is to the northeast of the depression's center and lies along the system's general track. Here, the bright band height is located around 5000 m and the freezing level is found near 4500 m. The range of storm heights varies from 6500 to 9000 m, again signifying a preponderance of nimbostratus cloud types. The cross-section (E) is ahead of the depression's main track and this cluster of precipitation is isolated from the main composite of depressions. The bright band height is near 4800 m with the freezing height around 4670 m. Several convective cell tops reached 13 000 m. The surrounding locations have storm heights ranging from 5600 to 7700 m.

Cross-section (F) depicts another isolated part of the monsoon depression, which is located east of the system's center. This cross-section shows a very good convective cell embedded within the overall precipitation. The bright banding occurs around a height of 4680 to 4780 m, and the freezing height is 4780 m. The main convective cell has a peak height of 18 120 m and the heights reach 15 600–16 100 m immediately surrounding this cell. A secondary convective cell extending to a height of 14 660 m is also present here. The northern end of this cross-section has storm heights ranging from 8300 to 11 000 m. To the south, heights are more modest at 6000 7100 m. Cross-section (G) is located just off the Indian west coast. This area contains bright banding roughly between 4740 and 4820 m and a freezing level near 4800 m. The storm heights are lower over this region, and are around 5430 m, but higher sections also have been noted extending to 8600 m.

Cross-section (H) is along the coastal boundary along the coast of southwest India along the Western Ghats. As stated previously, some orographic precipitation is discernable on this cross-section. A unique feature of this cross-section is the absence of bright banding in this location. In isolated locations, a freezing height around 4750 m is found, and storm heights range from 5500 to 6500 m. This reflects the more scattered nature of the precipitation in this location.

Cross-section (I) is located in the left-front quadrant of the system and shows several convective peaks. The bright banding is limited here due to a preponderance of convective systems. Isolated bright banding is generally found around 5000 m over this region. The freezing level is found near 4800 m. The peak cells in this area are around 12 000–15 000 m. In addition, the surrounding areas the storm heights are distributed between 7500 and 9000 m, indicating a prevalence of convective systems in this section.

Cross-section (J) is along a northwest to southeast line through the center of the composite monsoon depression. At 4600–4800 m the bright banding is seen with a freezing height of 4750 m. A band of convective systems with heights of the order of 8500 m are found to the eastern side of the composite depression. The convective cell has a maximum peak at 13 000 m. Surrounding these areas, storm heights generally reach from 5100 to 7300 m. Cross-section (K) is located parallel to the Indian eastern coast and makes up the eastern edge of the left-front quadrant of the monsoon depression. The bright banding is around 4670–4980 m, and the freezing height is at 4850 m. The main cell of this section has a storm height near 17 100 m, with secondary peaks from 12 240 to 13 400 m. Surrounding these convective systems, the storm heights range from a low of 5600 m to a high of 8600 m.

5. Discussion

When we examine the precipitation distributions around the composite monsoon depression, shown in Fig. 4, we see rainfall amounts covering a range of values: blue, 10–20 mm d^{-1}; green, 20–30 mm d^{-1}; yellow, 30–40 mm d^{-1}; and red, >50 mm d^{-1}. Previous studies on heavy rain in excess of 50 mm d^{-1} were generally assumed to be occurring from tall cumulonimbus clouds (Rao, 1976). As we look at the vertical cross section of the radar reflectivities in Fig. 4, we note that most heavy rains, sections D, F and G do not exhibit the presence of tall clouds. Over these land areas, surface weather reports generally provide a plethora of nimbostratus cloud distributions. These radar cross-section confirm that much of the rain occurring in a monsoon depression is stratiform. Tall clouds are in a few of these vertical cross-sections, such as section J in the vicinity of the storm center, orographic ascent regions in section K and offshore convection in section F.

The bright banding, seen in most cross-sections, appears to have a few hundred metres depth located around 4700 m. Thus warm rain from layer clouds is a strong contribution over these regions. In those few instances where great vertical depth was clearly apparent, signifying deep cumulonimbus convection, we were able to identify cells extending from 12 to 17 km.

This view of the monsoon depression was not possible in previous studies (Raghavan et al., 1983), since most ground-based Doppler radar units were deployed only over coastal areas for tropical cyclone surveillance. The TRMM radar provided a first opportunity to examine these structures over interior land areas. Another interesting matter to note here is that, although rainfall amount in the composite depression only ranged from 10 to 100 mm d^{-1}, the size of this disturbance is of the order of 3000 km and has a phase speed of 750 km d^{-1}; thus the total rainfall amount during the passage of the disturbances (roughly 3–4 d at any location) results in a large total rainfall amount of the order of 200 mm.

6. Conclusions and future work

A monsoon depression spends much of its life over the land area of the Indian subcontinent. Lacking land-area ground-based radar units over central India, it has been difficult to map the precipitation and vertical distribution of hydrometeors during the passage of a monsoon depression. Ground-based radar units have provided some information on the hydrometeor structure of these storms over the coastal regions (Raghavan, 1983); however, not much is known on the precipitation structure over the land area. In this study we have exploited the use of satellite-borne radar (TRMM-PR) to attempt to map these features. The PR provides the same resolution (4.3 km) as ground-based Doppler radar. Kummerow et al. (2000) alluded to the potential of TRMM radar, having calibrated this radar with several ground-based radar units. This satellite-borne radar was in turn used to calibrate a number of remote ground-based radar units over the tropical countries. Using some 16 orbits of flights over the Indian subcontinent it became possible to obtain a composite radar structure from three monsoon depressions for 1999.

What we have learned here is that we can obtain a fine structure on the areal distribution of precipitation for the monsoon depression. That appears to hold more detail than it has been possible to obtain from the indirect estimates received from OLR- and SSM//I-based data sets. The new aspect of this study is the display of vertical structure diagrams around the monsoon depression. Here we confirm the preponderance of stratiform rain and the coverage of fewer deep convective elements. That is not surprising, considering that the tropical upper tropospheric easterly jet (Koteswaram, 1958) draws out extended anvils from the few cumulonimbus clouds that reside within the monsoon depression. The analysis of the radar cross-section confirms the preponderance of nimbostratus clouds in this environment that has been known from surface reports. The sharp well defined melting layers topping at around 6000 m are a common feature over land depressions. Rainfall rates are largest in the front right quadrant (to the north east of a westward moving storm): these values are of the order of 25–30 mm d^{-1}. Looking around the monsoon depression, we see that on its horizontal scale of roughly 3000 km, it is primarily driven by some seven tall cumulonimbus cloud elements. These disturbances generally carry a cold core in the lower troposphere, where the thermal structure is maintained by the evaporation of falling rain and the adiabatic ascent. A weak warm core thermal structure caps this cold core structure, where the latent heat release is an important contributor to its maintenance (Krishnamurti et al., 1975).

Further work is possible to composite the life cycle of a monsoon depression from its origins over the Bay of Bengal to its eventual demise over the foothills of the Himalayas. Since the TRMM has continued to operate for several years now (it was launched in late 1997), it should be possible to provide such extensions.

7. Acknowledgements

The research reported here was supported by a NOAA grant NA96GPO400 and a NASA grant NAGS-9662.

REFERENCES

Awaka, J., Iguchi, T. and Okamoto, K. 1998. Early results on rain type classification by the Tropical Rainfall Measuring Mission (TRMM) precipitation radar. In *Proc. 8th URSI Commission F Open Symp.*, Aveiro, Portugal, pp. 143–146.

Bedekar, V. C. and Banerjee, A. K. 1969. A study of climatological and other rainfall patterns over central India, Indian. *J. Geophys.* **20**, 23–30.

Ferraro, R. R., Smith, E. A., Berg, W. and Huffman, G. J. 1998. A screening methodology for passive microwave precipitation retrieval algorithms. *J. Atmos. Sci.* **55**, 1583–1600.

Godbole, R. V. 1973. Numerical simulation of the Indian summer monsoon, *Ind. J. Meteorol. Geophys.* **24**, 1–13.

Godbole, R. V. 1977. The composite structure of the monsoon depression. *Tellus* **29**, 25–40.

Houze, R. A. 1997. Stratiform precipitation in regions of convection: a meteorological paradox? *Bull. Am. Meteorol. Soc.* **78**, 2179–2196.

India Meteorological Department (IMD). 2000. Cyclones and depressions over north Indian Ocean during 1999. *Mausam* **51**, 215–224.

Koteswaram, P. 1958. The easterly jet stream in the tropics. *Tellus* **10**, 43–57.

Kozu, T., Kawanishi, T., Kuroiwa, H., Kojima, M., Oikawa, K., Kumagai, H., Okamoto, K., Okumura, M., Nakatsuka, H. and Nishikawa, K. 2001. Development of precipitation radar onboard the Tropical Rainfall Measuring Mission (TRMM) satellite. *IEEE Trans. Geosci. Remote Sensing* **39**, 102–116.

Krishnamurti, T. N., Kanamitsu, M., Godbole, R., Chang, C. B., Carr, F. and Chow, J. H. 1975. Study of a monsoon depression (I): synoptic structure. *J. Meteorol. Soc. Jpn.* **53**, 227–240.

Krishnamurti, T. N., Kishtawal, C. M., Shin, D. W. and Williford, C. E. 2000. Multimodel superensemble forecasts for weather and seasonal climate. *J. Climate* **13**, 4196–4216.

Kummerow, C., Olson, W. S. and Giglio, L. 1996. A simplified scheme for obtaining precipitation and vertical hydrometer profiles from passive microwave sensors. *IEEE Trans. Geosci. Remote Sens.* **34**, 1213–1232.

Kummerow, C., Simpson, J., Thiele, O., Barnes, W., Chang, A. . C., Stocker, E., Adler, R. F., Hou, A., Kakar, R., Wentz, F., Ashcroft, P., Kozu, T., Hong, Y., Okamoto, K., Iguchi, T., Kuroiwa, H., Im, E., Haddad, Z., Huffman, G., Ferrier, B., Olson, W. S., Zipser, E., Smith, E. A., Wilheit, T. T., North, G., Krishnamurti, T. N. and Nakamura, K. 2000. The status of the Tropical Rainfall Measuring Mission (TRMM) after two years in orbit. *J. Appl. Meteorol.* **39**, 1965–1982.

Liu, G. and Fu, Y. 2001. The characteristics of tropical precipitation profiles as inferred From satellite radar measurements. *J. Meteorol. Soc. Jpn.* **79**, 131–143.

Meneghini, R., Kumagai, H., Wang, J. R., Iguchi, T. and Kozu, T. 1997. Microphysical retrievals over stratiform rain using measurements from an airborne dual-wavelength radar radiometer. *IEEE Trans. Geosci. Remote Sensing* **35**, 487–506.

Raghavan, S., Sivaramakrishnan, T. R. and Ramakrishnan, B. 1983. Size distribution of radar echoes as an indicator of growth mechanisms in monsoon clouds around Madras. *J. Atmos. Sci.* **40**, 428–434.

Rao, Y. P. 1976. *Southwest Monsoon.* India Meteorological Department, Meteorological Monograph, Synoptic Meteorology, No. 1/1976, 367 pp.

Short, D. A. and Nakamura, K. 2000. TRMM radar observations of shallow precipitation over the tropical oceans. *J. Climate* **13**, 4107–4124.

Simpson, J., Adler, R. F. and North, G. R. 1988. A proposed Tropical Rainfall Measuring Mission (TRMM) satellite**.** *Bull. Am. Meteorol. Soc.* **69**, 278–278.

Steiner, M., Houze, R. A. Jr. and Yuter, S. E. 1995. Climatological characterization of three-dimensional storm structure from operational radar and rain gauge data. *J. Appl. Meteorol.* **34**, 1978–2007.

TRMM Science Operations Plan, 1996. Copy available from TRMM website (trmm.gsfc.nasa.gov/publications_dir/sciencedoc.html)

Xie, P. and Arkin, P. A. 1998. Global monthly precipitation estimates from satellite-observed outgoing longwave radiation. *J. Climate* **11**, 137–164.